Interactions between polystyrene nanoparticles and Chlamydomonas reinhardtii monitored by infrared spectroscopy combined with molecular biology

Maureen Déniel, Nicolas Errien, Fabienne Lagarde, Marie Zanella, Aurore Caruso

▶ **To cite this version:**

Maureen Déniel, Nicolas Errien, Fabienne Lagarde, Marie Zanella, Aurore Caruso. Interactions between polystyrene nanoparticles and Chlamydomonas reinhardtii monitored by infrared spectroscopy combined with molecular biology. Environmental Pollution, 2020, 266, pp.115227. 10.1016/j.envpol.2020.115227 . hal-03324542

HAL Id: hal-03324542
https://hal.science/hal-03324542

Submitted on 22 Aug 2022

HAL is a multi-disciplinary open access archive for the deposit and dissemination of scientific research documents, whether they are published or not. The documents may come from teaching and research institutions in France or abroad, or from public or private research centers.

L'archive ouverte pluridisciplinaire **HAL**, est destinée au dépôt et à la diffusion de documents scientifiques de niveau recherche, publiés ou non, émanant des établissements d'enseignement et de recherche français ou étrangers, des laboratoires publics ou privés.

Distributed under a Creative Commons Attribution - NonCommercial 4.0 International License

Version of Record: https://www.sciencedirect.com/science/article/pii/S0269749120318169
Manuscript_d0802363f20e45a707b93df3e16b0db6

Interactions between polystyrene nanoparticles and *Chlamydomonas reinhardtii* monitored by infrared spectroscopy combined with molecular biology

Authors: Maureen Déniel[a], Nicolas Errien[a], Fabienne Lagarde[a], Marie Zanella[b], Aurore Caruso[b]*

[a] Le Mans Université, IMMM UMR-CNRS 6283, Avenue Olivier Messiaen, 72085 Le Mans Cedex 9, France

[b] Laboratoire Mer, Molécules, Santé, EA 2160, Avenue Olivier Messiaen, 72085 Le Mans Cedex 9, France

maureen.deniel@univ-lemans.fr (https://orcid.org/0000-0001-8374-3624) ; nicolas.errien@univ-lemans.fr, (https://orcid.org/0000-0001-9806-2258);

fabienne.lagarde@univ-lemans.fr (https://orcid.org/0000-0002-4015-4376);

marie.zanella@univ-lemans.fr

* Corresponding author: aurore.caruso@univ-lemans.fr (https://orcid.org/0000-0002-4327-543X), +33 (0)2 43 83 26 80, Laboratoire Mer, Molécules, Santé, EA 2160, Avenue Olivier Messiaen, 72085 Le Mans Cedex 9, France

Abstract

For several decades, use of nanoparticles (NP) on a global scale has been generating new potential sources of organism disruption. Recent studies have shown that NP can cause modifications on the biochemical macromolecular composition of microalgae and raised questions on the toxicity of plastic particles, which are widespread in the aquatic environment. Polystyrene (PS) particles are among the most widely used plastics in the world. In our experimentation, a combined approach of infrared spectroscopy and molecular biology (real-time PCR) has been applied in order to better apprehend the consequences of interactions between *Chlamydomonas reinhardtii*, freshwater microalgae and PS NP. Two references have been used, nitrogen deprivation -a well-documented stressor-, and gold nanoparticles (Au-NP). As regards biochemical

© 2020 published by Elsevier. This manuscript is made available under the CC BY NC user license
https://creativecommons.org/licenses/by-nc/4.0/

composition, our experiments show a differing microalga response, according to the NP to which they have been exposed. Results with infrared spectroscopy and gene expression methods are consistent and illustrate variation among several carbohydrates (galactose...). Furthermore, PS-NP seem to react in the same direction as nitrogen limitation, thereby supporting the hypothesis that PS-NP can induce response mechanisms to environmental changes in microalgae. This study highlighted the interest of combining infrared spectroscopy and gene expression as means of monitoring microalgae response to nanoplastics.

Keywords: Nanoplastics, microalgae, infrared spectroscopy, gene expression

Introduction

Nanomaterials are ubiquitous in the environment (Robichaud et al., 2009); especially in aquatic systems. For several decades, nanoparticle (NP) use on a global scale has been generating new sources potentially adverse effects on organisms (Bergami et al., 2017; López-Serrano et al., 2014; Miller and Wickson, 2015). Recent studies have shown that NP can generate modifications of macromolecular microalgae composition. For example, in the presence of titanium nanoparticles, Sadiq et al. (2011) observed a decrease of microalgae *Chlorella* and *Scenedesmus* sp. chlorophyll content. Among the models available for study of the impact of environmental changes on the aquatic systems, microalgae are ideal. The unicellular organisms and primary producers' responses to natural changes (lack in nutrients, ion presence and light fluctuations) are well documented (Irihimovitch and Yehudai-Resheff, 2008; Nama et al., 2015; Szivák et al., 2009). On the other hand, potential stresses caused by interactions with nanoparticles are not fully understood and seem to depend on diverse factors such as size, nature, shape, aggregation... (Tang et al., 2017). However, an increasing number of publications on the impact of this type of particle on the lives of organism have been compiled (von Moos and Slaveykova, 2014). There exist a wide variety of NP types, with metallic particles such as gold accounting for a sizable portion (Déniel et al., 2019). The gold nanoparticles (Au-NP) used in biomedical applications are referenced in the literature as non-toxic

elements (Alkilany and Murphy, 2010; Fratoddi et al., 2015). Other nanoparticles such as nanoplastics, of which the presence in aquatic environment is problematical, were detected by Ter Halle et al. (2017). However, their interactions with aquatic organisms have not been extensively described, and only a limited number of commercially available products have been studied (Besseling et al., 2014; Bhattacharya et al., 2010; Casado et al., 2013; Li, 2015; Sjollema et al., 2016). Furthermore, the toxicity of plastic nanoparticles has been called into question, as some articles have indicated a fluctuation of effects according to the surfactant at the particle surface (Bergami et al., 2017; Nolte et al., 2016). To understand how nanoplastics may enhance stress or toxicity in organism, it has become necessary to more clearly specify the responses of microalgae and the different types of NP-microalgae interactions. Different types of interactions have been reported in the literature: shading effect, adsorption, absorption, endocytosis, aggregation, cell-wall disruption, ion release… (Moore, 2006; Navarro et al., 2008; von Moos and Slaveykova, 2014). They generate specific biologic responses leading to morphological, biochemical or molecular changes in microalgae. In order for these responses to be clearly discerned, it is important to use repeatable, reliable, rapid and inexpensive methods.

To monitor biochemical composition, infrared microspectroscopy is a rapid and non-destructive analysis technique, which is known to facilitate detection of environmental stress (Dean et al., 2008; Déniel et al., 2020). Given the sensitivity of this technique to functional group conformational changes (C-O, N-H bonds…), it is interesting as a means of analyzing the sub-lethal effects of microalgae. Infrared spectroscopy was previously described as a useful tool to detect protein and carbohydrate variations in cases of nutrient starvation (Driver et al., 2015; Jakob et al., 2007; Stehfest et al., 2005) and, more recently, to follow microalgae under different stress conditions (Déniel et al., 2020). In addition, this technique facilitates monitoring of metabolite spatial distribution variation, as has been shown for *Micrasterias hardyi* after exposure to active pharmaceutical ingredients (Patel et al., 2008). Infrared spectroscopy has also been used to study

cellular carbon allocation according to phosphorus quota in *Chlamydomonas reinhardtii* (Dean et al., 2008).

Biochemical changes, particularly those linked to the biosynthesis pathway of proteins or enzyme variations, are the result of modifications at the molecular level. To better understand macromolecular microalgae variations, gene expression analysis can be followed by Q-RT-PCR (quantitative Reverse Transcription - Polymerase Chain Reaction). Following microalga-microplastic interactions, this method has been applied in study of the metabolic pathway of carbohydrate biosynthesis in *Chlamydomonas reinhardtii* (Lagarde et al., 2016). Xylose, glucose, galactose and rhamnose are polysaccharides characterized by GC–MS analysis in *C. reinhardtii* (Bafana, 2013). Moreover, some sugars are recognized as participating in stress response, one example being sulphated polysaccharides, in *C. reinhardtii*, which has antioxidant properties (Kamble et al., 2018).

Another article identified composition changes in monosaccharides consecutive to salt concentration variation in *Dunaliella salina* (Mishra and Jha, 2009) supporting the hypothesis of variations in polysaccharide content and given its implication in stress response, carotenoid gene expression has been studied (Couso et al., 2012; Wang et al., 2016).

This study describes a combined approach of infrared spectroscopy and Q-RT-PCR to monitor and highlights the consequences of interactions between *Chlamydomonas reinhardtii*, a freshwater microalga, and polystyrene nanoparticles. Two other stresses are used as references in these experiments, nitrogen deprivation (N-less), - a stress factor that is well- documented as affecting the growth and biochemical composition of microalgae (Gargouri et al., 2017; Park et al., 2015; Schmollinger et al., 2014; Zarrinmehr et al., 2019), and gold nanoparticles (Au-NP) (Lapresta-Fernández et al., 2012; Pal et al., 2011).

Materials and methods

Nanoparticle characteristics

The nanoparticles used are 100 nm nanobeads commercialized by Interchim. Au-NP are in an aqueous solution at a concentration of 0.01% with a citrate surfactant. The polystyrene nanoparticles (PS-NP) are stabilized with an anionic surfactant in aqueous solution at 1% concentration. Zeta potential and size of nanoparticles in culture medium are measured with a Zetasizer Nano ZS device (Malvern).

Culture conditions

Chlamydomonas reinhardtii (strain 2935, *Chlamydomonas* Resource Center, (Sack et al., 1994)) is cultivated in 250 mL Erlenmeyer containing 70 mL of Tris Acetate Phosphate medium (TAP medium) (Gorman and Levine, 1965) at 20°C. The Erlenmeyer flasks are placed under an irradiance of 122 µmol photons.m^{-2}.s^{-1}. Lighting is provided by cool white fluorescent tubes (Philips TLD 36 W) and follows a light/dark cycle of 14/10 hours. Cultures are kept in suspension by agitation at 100 rpm (VWR, Model 5000).

C. reinhardtii (1*10^6 C/mL in the beginning of the experiment) are subjected to various environmental variations for 8 days. Each condition is produced in triplicate with a control group on which no stress is applied. The two types of nanoparticles are interacted separately with microalgae: Au-NP (2 mg/L, either 143 mmol/L or 7.1*10^5 NP/microalgae) and PS-NP (2 mg/L, either 274 mmol/L or 13.1*10^6 NP/microalgae). In congruence with literature on PS-NP interactions, where tested concentrations ranged between 0.1 and 50 mg/L, a concentration of 2 mg/L PS-NP was chosen (Bergami et al., 2017; Casado et al., 2013; Nolte et al., 2016). Nitrogen (N-less) intake is reduced by 15% compared to the control group (a concentration of 6 mM N in medium vs. 7 mM normally). Microalgae growth is measured by cellular counting on Malassez cells.

Infrared spectroscopy

Infrared spectra acquisition is carried out in triplicate on microalgae drops of 10 µL for each tested condition, after one hour of air drying (Dean et al., 2008) of samples on a double-side polished silicon wafer. The transmission mode of the infrared spectroscope (Vertex IR 70v, Bruker) is applied, with an accumulation of 50 scans from 4000 to 500 cm^{-1} and a resolution of 4 cm^{-1}.

On raw spectra, preprocessing of the linear baseline (LB) with a standard normal variate (SNV) is applied to normalize each data group to allow relative quantification of functional bonds. SNV removes multiplicative scattering interferences by zero centering and scaling of individual spectra. The whole spectrum is centered on its mean, and whole intensity is adjusted with the standard deviation. Study analysis ranges from 800 to 1780 cm^{-1}. Multivariate analysis of data using PCA (principal component analysis) is carried out successively to preprocessing with the study of loadings.

To explore the carbohydrate bands in more detail, peak deconvolution of the 930-1190 cm^{-1} zone is carried out with PeakFit v4.02 software. During this Gaussian-Lorentzian area deconvolution, 6 peaks (980, 1018, 1049, 1078, 1108 and 1152 cm^{-1}) are used to fit the band with half-height width considered as the same for each peak referenced. Minimal R^2 accepted to fit is 0.99. After peak deconvolution, area percentage contribution is calculated for each peak of the whole massif band.

Molecular biology: RNA extraction, and quantification-RT-PCR

Ten mL of culture in each condition are filtered (Whatman glass microfiber filters, 47 mm diameter, 1.2 µm pore size). RNA is extracted using a Spectrum Plant Total RNA kit (Sigma-Aldrich, Saint Louis, USA). Sample purity and RNA concentration assay are obtained by deposition of 1 µL on a Nanodrop 2000 (Thermo Scientific).

All RNA samples are subsequently standardized to a concentration of 100 ng/µL to perform a reverse transcriptase according to MMLV kit instructions (Promega, Madisson, USA) in presence

147 of 5 µM oligodT_{VN} modified, (Carpin et al. 1998), 25.5 µM random primers (8-10 pb), 2.5 x
148 MMLV Buffer, 0.5 mM dNTP, 25 U RNAse inhibitor and 200 U MMLV enzyme. The reaction is
149 carried out in a thermocycler (Applied Biosystems Veriti 96-Well Programmable Thermocycler), in
150 two phases: 5 min at 70 °C and one hour at 42 °C. Quantitative PCR (Q-PCR) is also carried out in
151 two steps, using a StepOne-plus Real-Time thermocycler (Applied Biosystems) with SYBER-Green
152 Q-PCR Master Mix (Promega, Madisson, USA).

153 Seven target genes (five involved in polysaccharides biosynthesis and two in carotenoid
154 biosynthesis) are selected in accordance with previous work (Couso et al., 2012; Lagarde et al.,
155 2016; Wang et al., 2016) and primer sequences were designed with Primer3-Plus software
156 (http://www.bioinformatics.nl/cgi-bin/primer3plus/primer3plus.cgi). Choice of genes for the sugar
157 biosynthetic pathway was carried out according to those known in the literature and the sequence of
158 which is available in the databases (https://genome.jgi.doe.gov/portal/). Efficiency and melting
159 curves for each primer pair (Table 1) were produced on cascade dilutions of a cDNA mixing. The
160 1:8 dilution and the primers with optimal efficiency range of 85%-111% were selected for the
161 second phase of Q-PCR. The Ct (threshold cycle) comparison method (Livak and Schmittgen,
162 2001) was applied to calculate the gene expression level. Housekeeping genes, rps2 and rps14,
163 presenting the best stability among tested conditions, were selected with Best Keeper software
164 (Pfaffl et al., 2004) and used for normalization of the gene expression studied. Gene expression
165 level (EL) was calculated from Ct of each sample: ($EL = ((E_{TG})^{\Delta Ct\ TG}) / (E_{HG})^{\Delta Ct\ HG}$), (TG: Target
166 Gene; HG: Housekeeping Gene; $\Delta Ct = Ct_{Control} - Ct_{Sample}$). Amplification program consisted of 15 s at
167 95 °C followed by 35 cycles of one minute to decrease to 60 °C.

168

169

170

Table 1 : List of genes tested and primer sequences: housekeeping gene (rps 2, 8, 14, 19), genes involved in the biosynthesis pathway of sugars (GD, GE, GLD, ME, PG), astaxanthin biosynthesis pathway genes (BKT, CHY)

Complete gene name	Short gene name	Forward/ Reverse	Primer sequences 5'=> 3'
ribosomal protein, small unit 2	rps 2	F	CGAACGGTAAAGAAAATGCT
		R	ACAAATTGCAGCCCAAAAAC
ribosomal protein, small unit 8	rps 8	F	TCGCCTTAAATATCGTTCAAAA
		R	CCTTCAGGCGTTGTTAAACAAT
ribosomal protein, small unit 14	rps 14	F	ACGGTTGTGTAACGACTG
		R	GCGTGAATTAAACGCCAAA
ribosomal protein, small unit 19	rps 19	F	CACGTTCATCAATGATTGTTCC
		R	TTAGCATGGCCACGATATGTA
UDP-glucoronate decarboxylase, xylose	GD	F	GTGACTACCTGGTGGCTCGT
		R	GATTTGGTCCACCTCCAAGA
UDP glucose 4 epimerase, galactose	GE	F	CAAGCCGCTCGAGTACTACC
		R	ACATGTCCTCCTGGAACAGC
UDP glucose 4-6dehydratase, rhamnose	GLD	F	CATCAAGGGCGATATCCAGT
		R	GGTCTCGCCATACACCTCAT
GDP mannose 3-5 epimerase, galactose	ME	F	GTCCTTCGACGACAAGAAGC
		R	TGCTGTGGCTGTACTTGGTT
Phosphoglucomutase glucose	PG	F	CGACCGTGTTATTTGCCTTCG
		R	GGTCTCGCCATACACCTCAT
β-carotene hydrolase astaxanthin biosynthesis pathway	CHY	F	GAGCTCAACGACATCTACGC
		R	TTGGTGTGGTGGATCTGATG
β-carotene ketolase astaxanthin biosynthesis pathway	BKT	F	TTCCGCCTGTTCTACTACGG
		R	GTGCTCCCAGTGCAGGTC

Statistical tests (Shapiro for normality, Levene for homoscedasticity, ANOVA and HSD test of Tukey if data were normal and homogeneous, otherwise Kruskall-Wallis and Wilcoxon) were carried out with R software (v 3.4.4) on each gene to control significant differences (at 5%) in answers among diverse conditions.

Results and discussion

Nanoparticle characterization

Au-NPs have a size of 190 nm and a zeta potential of -14 mV. PS-NsP have a hydrodynamic diameter of 158 nm and a zeta potential of -50 mV (Supplementary data Figures S1 and S2).

Infrared spectroscopy of microalgae and PCA analysis

After 8 days in interaction with PS and Au-NP and 8 days in control and N-less conditions, mean raw infrared spectra of *C. reinhardtii*, are determined (Figure S3). The spectra display linear baseline preprocessing and standard normal variate (LB+SNV) (Figure 1).

First, a peak offset on protein band (N-H) is observed at 1540 cm^{-1} for microalgae infrared spectra under N-less exposure (Figure 1). For the 1110 cm^{-1} peak (elongation vibration, vC-O) of carbohydrates, absorbance variation was observed with differentiation of the Control and Au-NP group on the one hand and PS-NP and N-less on the other hand. In our study conditions, PS-NP and N-less conditions could then be considered as stressors. As was the case with salt stress in *Dunaliella salina* (Mishra and Jha, 2009), they generated carbohydrates content variation.

However, the PCA derived (Figure 2a) from the spectra of the 4 conditions showed that the N-less group was distinguished from the other three. A new PCA was performed for the three other conditions (Figure 2b), which display more similar spectra. PCA (Figure 2b) clearly separates the sample corresponding to the microalgae in contact with PS-NP from the two other groups. Microalgae in contact with Au-NP exhibit the same behavior as the Control sample. PCA loadings are presented in Figure 3. The principal component (PC1) explains 53% of spectral variation and presents a positive variation at 1109 cm^{-1}, which is attributed to the C-O chemical bond of carbohydrates (Murdock and Wetzel 2009; Coronado, Galán-Mascarós, and Martí-Gastaldo 2009 ; Figure 3a). Protein bands (C=O: 1659 cm^{-1} and N-H: 1547 cm^{-1}) showed a negative variation on PC1. The second component PC2 (40%), which mainly discriminates the PS-NP group from the two others, contains (see Figure 3b) bands at 1672 cm^{-1} (protein chemical bond C=O), 1109 cm^{-1} and 1034 cm^{-1} (carbohydrate chemical bond vC-O), 881 cm^{-1} (carbohydrate chemical bond C-H

(Liu et al., 2018; Umezawa and Komiyama, 1985)) and 816 cm^{-1} (chemical bond C-O-S, galactose sulfate in C6 (Ananthi et al., 2010; Chopin and Whalen, 1993)). A protein peak shift (1659 cm^{-1} to 1672 cm^{-1}) between the two principal component loadings underlined a chemical or physical environment modification (Figure 1 and Figure 3). PC3 is not very relevant insofar as it reflects only 3% of the variations (Figure 3c).

The fact that Au-NP and Control conditions do not differ seems to support use of Au-NP as non-toxic standard (Connor et al., 2005). Nature and surface chemistry of particles are potential factors affecting interaction modes (Stone et al., 2010). In this study, although the concentration tested in Au-NP was higher than in previous studies (Dědková et al., 2014; Moreno-Garrido et al., 2015), this did not lead to significant variation in the biochemical composition of microalgae compared to the control. Moreover, Au-NP toxicity has been discussed in the literature and, after size, surfactant nature could be a more important factor of particle toxicity (Moreno-Garrido et al., 2015).

The main variations observed with PS-NP were linked to the protein and carbohydrate bands and may have been influenced by the nature or surface chemistry of the nanoparticles. Moreover, it should be noted that the infrared bands related to carbohydrates (1200-900 cm^{-1}) represent a complex area of the microalgae spectrum (many peaks) on which it was necessary to carry out a detailed study. Carbohydrates are intertwined in the microalgae structure with other components in a complex chemical environment, leading to an overlap of carbohydrates bands in infrared spectra.

Analysis of infrared spectra 1190-930 cm^{-1} range: carbohydrate bands

A more in-depth analysis of all the carbohydrate bands was carried out by spectral deconvolution of the average spectra of *C. reinhardtii* obtained for each condition using six components (based on spectra shape and half-height width). The spectral deconvolution method provides satisfactory resolution of absorption bands in carbohydrate study according to Buslov et al.

(2000) and Palmucci et al. (2011). Figure 4 presents deconvolution and the area percentage of the six peaks describing the bonds of the carbohydrates. First, as in PCA (Figure 2b), very few differences between the distribution of the bands in control and Au-NP conditions (Figure 4 a and b) are observed. This finding once again highlights the use of gold as the standard for inert nanoparticles. With regard to the PS-NP and the N-less conditions, similar variations are observed Figure 4c and d). A decrease is noted in the percentage of area of the 1108 cm^{-1} band corresponding to v(C-O) of carbohydrates (Wiercigroch et al., 2017) in the two conditions and a decrease of 1152 cm^{-1} (C-O-C glucose conformation, (Nikonenko et al., 2000), with a peak contribution for N-less only. In parallel, Figure 4c and d, show an increase in the contribution of the peak to 1018 cm^{-1} (corresponding to v(C-O), (Duygu et al., 2012), which is much greater in N-less condition compared to NP, and relatively similar for the peaks at 1078 cm^{-1}, which according to Wiercigroch et al. (2017), are related to v (C-O) and at 1049 cm^{-1} (C-OH, (Hofman and Witanowski, 1959)). The proportions of 980 cm^{-1} peaks (β(C-CH), β(C-CO) linked to fructose (Wiercigroch et al., 2017)) remain relatively stable compared to the control group, meaning that fructose content does not fluctuate in the event of nutrient stress or nanoparticle interaction. Variations of bands corresponding mainly to carbohydrates are observed, but only a few are clearly identified with a specific carbohydrate present in *C. reinhardtii*. With infrared spectroscopy data alone it is consequently difficult to assign a specific carbohydrate type to each band.

Responses of genes linked with carbohydrates

In an attempt to identify the carbohydrates having fluctuated, gene expression monitoring of the carbohydrate biosynthesis pathway was carried out. Variations of gene expression linked with carbohydrates were previously reported under cold stress (5°C) in *C. reinhardtii*, showing overexpression of the sucrose-phosphate-synthase and trehalose-6-phosphate synthase 1 genes implicated in sucrose and trehalose biosynthesis respectively (Valledor et al., 2013). In addition, carbohydrate variations of *C. reinhardtii* were reported under low illumination, with

253 underexpression of hexose kinase (glycolysis) and α-trehalase (glucose dimer cleavage) (Puzanskiy
254 et al., 2018). Moreover, Lagarde et al. (2016) have shown overexpression of two genes linked with
255 biosynthesis pathways: galactose and xylose in the presence of microplastic particles
256 (polypropylene and high-density polyethylene).

257 The gene expression levels of the biosynthetic pathway of four sugars (glucose, xylose,
258 rhamnose and galactose) were evaluated by real time RT-PCR. First, the biosynthesis pathway
259 corresponding to the glucose is monitored via phosphoglucomutase (PG) expression. The gene
260 encoding the UDP-glucoronate decarboxylase enzyme (GD) is implicated in the xylose biosynthesis
261 pathway. The third gene monitored is that of the UDP glucose 4-6 dehydratase (GLD) involved in
262 rhamnose biosynthesis. Finally, with regard to galactose, the transcripts of two genes were
263 measured: UDP glucose 4 epimerase (GE) and GDP mannose 3-5 epimerase (ME). In addition, two
264 other genes, potentially stress markers, encoding enzymes of the astaxanthin biosynthesis pathway,
265 were monitored: β-carotene ketolase (BKT) and β-carotene hydrolase (CHY) (Huang et al., 2012).
266 Figure 5 presents the relative expressions for the genes in the different conditions. Expression of the
267 two genes linked with the astaxanthin biosynthesis pathway was used to follow the response to
268 stress: BKT gene, an enzyme known to catalyze a limited number of steps for astaxanthin synthesis
269 and CHY gene, an enzyme implicated in changeover of β-carotene in astaxanthin (Huang et al.,
270 2012). Under-expression of BKT and CHY gene is observed in *C. reinhardtii* after interaction with
271 PS-NP and N-less. A study on *Haematococcus pluvialis* also showed under-expression of these two
272 genes under light stress (Lee et al., 2018). This result suggests that PS-NP presence can be stressful
273 for *C. reinhardtii*. A gene linked with glucose synthesis (PG) is discriminatory to distinguish
274 particular effect (Au-NP) from plastic effect (PS-NP), since in the first case, overexpression is
275 observed, while in the second case, underexpression occurs (gene expression is 10 times lower than
276 control). Concerning GD genes linked with xylose synthesis, a N-less condition outlines
277 underexpression of 2.5 times. N-less and PS-NP conditions present underexpression compared to
278 control condition for rhamnose and glucose biosynthesis pathway genes. Likewise, underexpression

279 of two genes implicated in the biosynthesis pathway of galactose for PS-NP and N-less conditions
280 is also observed for GE gene linked equally to galactose biosynthesis pathway for the Au-NP
281 condition. In contrast, with glucose the gene linked to its expression is overexpressed in the Au-NP
282 group. It is also possible to differentiate the two types of nanoparticles by their differential
283 expression for mannose epimerase (ME) gene: microalgae in contact with Au-NP did not show
284 modified expression, whereas microalgae in contact with PS-NP presented under-expression of this
285 gene, 8 times less than the control.

286 Composition change in carbohydrates following an environmental change has been explored
287 in a green microalga, *Dunaliella salina*, which is close to our model. It was shown that the
288 exopolysaccharides (EPS) produced in saline stress were composed of monosaccharides: glucose
289 and galactose (aldohexose), fructose (hetohexose) as well as xylose (pentose) (Mishra and Jha,
290 2009). In our study, N-less condition is differentiated from other conditions by under-expression on
291 the majority of studied genes (PG, GE, GLD and BKT).

292 If we combine infrared data (Figure 2) with gene expression results (Figure 5), some
293 conclusions can be put forward. Wiercigroch et al. (2017) illustrated infrared band spectra
294 differences between hexose and pentose. If we observe gene expression (Figure 5), no variation of
295 linked with xylose, which is a pentose (Wiercigroch et al., 2017), was observed in the presence of
296 nanoparticles. On the contrary, glucose and galactose, which are hexoses, presented gene expression
297 variations in experiments with nanoparticles (GE and PG). In addition, under PS-NP and N-less
298 conditions, certain genes are underexpressed (GLD, ME, PG) in parallel with the decline at 1110
299 cm^{-1} of peak area portion and, for N-less, decline of the 1152 cm^{-1} peak only, linked with glucose.
300 In addition, if we refer to average infrared spectra (Figure 1), a decrease of the 1110 cm^{-1} band is
301 observed in association with a decrease of the bands at 881 and 816 cm^{-1}. The wavenumber at 816
302 is referenced according to Ananthi et al. (2010) and Chopin and Whalen (1993) as C-O-S chemical
303 bound of sulfate on C6 galactose. In parallel, underexpression of mannose epimerase (ME) gene is

observed. This result seems to highlight a correlation between molecular composition obtained by infrared and genetic expression of carbohydrates in *C. reinhardtii*.

Conclusion

The presence of nanoparticles in contact with microalgae causes a variation in *C. reinhardtii* biochemical composition. With the sensitive IR technique, the response of microalgae to nanoparticle can be discriminated. Microalgae in contact with AuNP have the same behavior as the Control sample (in IR spectra), thereby supporting the hypothesis that Au-NP can be a standard for inert nanoparticles in ecotoxicology. In presence of PS-NP or N-less, infrared spectroscopy spectra of *C. reinhardtii* showed a modification in protein and carbohydrate bands. In this study, an unmistakable implication of sugars in the PS-NP and *C. reinhardtii* interactions was likewise underlined, using spectral deconvolution. The infrared data are consistent with the gene expression results, which illustrate a variation of several carbohydrate biosynthesis pathways, including the gene related to galactose. As in principal component analysis, differentiation of the response between the two types of particles is highlighted (glucose and rhamnose at gene expression and infrared peak at 1110 cm^{-1}) by gene expression results. Furthermore, microalgae exposed to PS-NP show similarities of response with microalgae under N-less condition (GLD, ME, PG and 1110, 880 and 816 cm^{-1} linked with galactose), thereby supporting the hypothesis that polystyrene nanoparticles can induce microalgae response mechanisms under interactions.

Acknowledgments The authors would like to thank Frédéric Amiard for his technical assistance during infrared measurement and Jeffrey Arsham, an American translator, for his review of our original English-language text. Finally, we are grateful to “Spectroscopy” platform of *Institut Molécules et Matériaux du Mans* of Le Mans University for their technical support.

Funding information

328 This work was supported financially by Conseil Départemental de la Sarthe, Le Mans Métropole
329 and ANR CESA (ANR-15-CE34-0006-02, NANOPLASTICS project).

330 **Compliance with ethical standards**

331 **Conflict of Interest** The authors have no conflict of interest to declare.

332

References

Alkilany, A.M., Murphy, C.J., 2010. Toxicity and cellular uptake of gold nanoparticles: What we have learned so far? J. Nanoparticle Res. 12, 2313–2333. https://doi.org/10.1007/s11051-010-9911-8

Ananthi, S., Raghavendran, H.R.B., Sunil, A.G., Gayathri, V., Ramakrishnan, G., Vasanthi, H.R., 2010. In vitro antioxidant and in vivo anti-inflammatory potential of crude polysaccharide from *Turbinaria ornata* (Marine Brown Alga). Food Chem. Toxicol. 48, 187–192. https://doi.org/10.1016/j.fct.2009.09.036

Bafana, A., 2013. Characterization and optimization of production of exopolysaccharide from *Chlamydomonas reinhardtii*. Carbohydr. Polym. 95, 746–752. https://doi.org/10.1016/j.carbpol.2013.02.016

Bergami, E., Pugnalini, S., Vannuccini, M.L., Manfra, L., Faleri, C., Savorelli, F., Dawson, K.A., Corsi, I., 2017. Long-term toxicity of surface-charged polystyrene nanoplastics to marine planktonic species *Dunaliella tertiolecta* and *Artemia franciscana*. Aquat. Toxicol. 189, 159–169. https://doi.org/10.1016/j.aquatox.2017.06.008

Besseling, E., Wang, B., Lürling, M., Koelmans, A.A., 2014. Nanoplastic Affects Growth of S. obliquus and Reproduction of *D. magna*. Environ. Sci. Technol. 48, 12336–12343. https://doi.org/10.1021/es503001d

Bhattacharya, P., Sijie, L., James, P.T., Pu Chun, K., 2010. Physical Adsorption of Charged Plastic Nanoparticles Affects Algal Photosynthesis. J. Phys. Chem. C 114, 16556. https://doi.org/10.1021/jp1054759

Buslov, D.K., Nikonenko, N.A., Sushko, N.I., Zhbankov, R.G., 2000. Resolution enhancement in IR spectra of carbohydrates by deconvolution method and comparison of the results wit low temperature spectra. Appl. Spectrosc. 54, 1651–1658.

Casado, M.P., Macken, A., Byrne, H.J., 2013. Ecotoxicological assessment of silica and polystyrene nanoparticles assessed by a multitrophic test battery. Environ. Int. 51, 97–105.

https://doi.org/10.1016/j.envint.2012.11.001

Chopin, T., Whalen, E., 1993. A new and rapid method for carrageenan identification by FTIR diffuse reflectance spectroscopy directly on dried, ground algal material. Carbohydrates Res. 246, 51–59.

Connor, E.E., Mwamuka, J., Gole, A., Murphy, C.J., Wyatt, M.D., 2005. Gold nanoparticles are taken up by human cells but do not cause acute cytotoxicity. Small 1, 325–327. https://doi.org/10.1002/smll.200400093

Coronado, E., Galán-Mascarós, J.R., Martí-Gastaldo, C., 2009. Design of bimetallic magnetic chains based on oxalate complexes: Towards single chain magnets. CrystEngComm 11, 2143–2153. https://doi.org/10.1039/b910490a

Couso, I., Vila, M., Vigara, J., Cordero, B.F., Vargas, M.Á., Rodríguez, H., León, R., 2012. Synthesis of carotenoids and regulation of the carotenoid biosynthesis pathway in response to high light stress in the unicellular microalga *Chlamydomonas reinhardtii*. Eur. J. Phycol. 47, 223–232. https://doi.org/10.1080/09670262.2012.692816

Dean, A., Nicholson, J., Sigee, D., 2008. Impact of phosphorus quota and growth phase on carbon allocation in *Chlamydomonas reinhardtii*: an FTIR microspectroscopy study. Eur. J. Phycol. 43, 345–354. https://doi.org/10.1080/09670260801979287

Déniel, M., Errien, N., Daniel, P., Caruso, A., Lagarde, F., 2019. Current methods to monitor microalgae-nanoparticle interaction and associated effects. Aquat. Toxicol. 217, 105311. https://doi.org/10.1016/j.aquatox.2019.105311

Déniel, M., Lagarde, F., Caruso, A., Errien, N., 2020. Infrared spectroscopy as a tool to monitor interactions between nanoplastics and microalgae. Anal. Bioanal. Chem. https://doi.org/10.1007/s00216-020-02683-9

Driver, T., Bajhaiya, A.K., Allwood, J.W., Goodacre, R., Pittman, J.K., Dean, A.P., 2015. Metabolic responses of eukaryotic microalgae to environmental stress limit the ability of FT-IR spectroscopy for species identification. Algal Res. 11, 148–155.

https://doi.org/10.1016/j.algal.2015.06.009

Duygu, D. (Yalcin), Udoh, A.U., Ozer, T. (Baykal), Akbulut, A., Erkaya, I., Yildiz, K., Guler, D., 2012. Fourier transform infrared (FTIR) spectroscopy for identification of *Chlorella vulgaris* Beijerinck 1890 and *Scenedesmus obliquus* (Turpin) Kützing 1833. African J. Biotechnol. 11, 3817–3824. https://doi.org/10.5897/ajb11.1863

Fratoddi, I., Venditti, I., Cametti, C., Russo, M.V., 2015. How toxic are gold nanoparticles? The state-of-the-art. Nano Res. 8, 1771–1799. https://doi.org/10.1007/s12274-014-0697-3

Gargouri, M., Bates, P.D., Park, J.J., Kirchhoff, H., Gang, D.R., 2017. Functional photosystem maintains proper energy balance during nitrogen depletion in *Chlamydomonas reinhardtii,* promoting triacylglycerol accumulation. Biotechnol. Biofuels 10, 1–21. https://doi.org/10.1186/s13068-017-0774-4

Gorman, S.D., Levine, R.P., 1965. Cytochrome F and plastocyanin : their sequence in the photosynthetic electron transport chain of *Chlamydomonas reinhardtii.* Proc. Natl. Acad. Sci. 54, 1665–1669. https://doi.org/10.1104/pp.126.1.69

Hofman, W.U., Witanowski, M., 1959. The Infrared Spectra of Some Carbohydrates. Bull. l'académie Pol. des Sci. VII, 619–624.

Huang, J., Zhong, Y., Sandmann, G., Liu, J., Chen, F., 2012. Cloning and selection of carotenoid ketolase genes for the engineering of high-yield astaxanthin in plants. Planta 236, 691–699. https://doi.org/10.1007/s00425-012-1654-6

Irihimovitch, V., Yehudai-Resheff, S., 2008. Phosphate and sulfur limitation responses in the chloroplast of *Chlamydomonas reinhardtii*. FEMS Microbiol. Lett. 283, 1–8. https://doi.org/10.1111/j.1574-6968.2008.01154.x

Jakob, T., Wagner, H., Stehfest, K., Wilhelm, C., 2007. A complete energy balance from photons to new biomass reveals a light- and nutrient-dependent variability in the metabolic costs of carbon assimilation. J. Exp. Bot. 58, 2101–2112. https://doi.org/10.1093/jxb/erm084

Kamble, P., Cheriyamundath, S., Lopus, M., Sirisha, V.L., 2018. Chemical characteristics,

411 antioxidant and anticancer potential of sulfated polysaccharides from *Chlamydomonas*
412 *reinhardtii.* J. Appl. Phycol. 30, 1641–1653. https://doi.org/10.1007/s10811-018-1397-2
413 Lagarde, F., Olivier, O., Zanella, M., Daniel, P., Hiard, S., Caruso, A., 2016. Microplastic
414 interactions with freshwater microalgae: Hetero-aggregation and changes in plastic density
415 appear strongly dependent on polymer type. Environ. Pollut. 215, 331–339.
416 https://doi.org/10.1016/j.envpol.2016.05.006
417 Lapresta-Fernández, A., Fernández, A., Blasco, J., 2012. Nanoecotoxicity effects of engineered
418 silver and gold nanoparticles in aquatic organisms. TrAC - Trends Anal. Chem. 32, 40–59.
419 https://doi.org/10.1016/j.trac.2011.09.007
420 Lee, C., Ahn, J.W., Kim, J.B., Kim, J.Y., Choi, Y.E., 2018. Comparative transcriptome analysis of
421 *Haematococcus pluvialis* on astaxanthin biosynthesis in response to irradiation with red or
422 blue LED wavelength. World J. Microbiol. Biotechnol. 34, 1–14.
423 https://doi.org/10.1007/s11274-018-2459-y
424 Li, X., 2015. Interactions of silver and polystyrene nanoparticles with algae. École polytechnique de
425 Lausanne. https://doi.org/10.5075/epfl-thesis-6818
426 Liu, N., Wu, X., Fu, X., Duan, D., Xu, J., Gao, X., 2018. Characterization of Polysaccharides
427 Extracted from a Cultivated Brown Alga *Costaria costata* During the Harvest Period. J. Ocean
428 Univ. China 17, 1209–1217. https://doi.org/10.1007/s11802-018-3621-8
429 Livak, K.J., Schmittgen, T.D., 2001. Analysis of relative gene expression data using real-time
430 quantitative PCR and the $2^{-\Delta\Delta CT}$ method. Methods 25, 402–408.
431 https://doi.org/10.1006/meth.2001.1262
432 López-Serrano, A., Olivas, R.M., Landaluze, J.S., Cámara, C., 2014. Nanoparticles: a global vision.
433 Characterization, separation, and quantification methods. Potential environmental and health
434 impact. Anal. Methods 6, 38–56. https://doi.org/10.1039/C3AY40517F
435 Miller, G., Wickson, F., 2015. Risk Analysis of Nanomaterials: Exposing Nanotechnology's Naked
436 Emperor. Rev. Policy Res. 32, 485–512. https://doi.org/10.1111/ropr.12129

437 Mishra, A., Jha, B., 2009. Isolation and characterization of extracellular polymeric substances from
438 micro-algae *Dunaliella salina* under salt stress. Bioresour. Technol. 100, 3382–3386.
439 https://doi.org/10.1016/j.biortech.2009.02.006
440 Moore, M.N., 2006. Do nanoparticles present ecotoxicological risks for the health of the aquatic
441 environment? Environ. Int. 32, 967–976. https://doi.org/10.1016/j.envint.2006.06.014
442 Moreno-Garrido, I., Pérez, S., Blasco, J., 2015. Toxicity of silver and gold nanoparticles on marine
443 microalgae. Mar. Environ. Res. 111, 60–73. https://doi.org/10.1016/j.marenvres.2015.05.008
444 Murdock, J.N., Wetzel, D.L., 2009. FT-IR microspectroscopy enhances biological and ecological
445 analysis of algae. Appl. Spectrosc. Rev. 44, 335–361.
446 https://doi.org/10.1080/05704920902907440
447 Nama, S., Madireddi, S.K., Devadasu, E.R., Subramanyam, R., 2015. High light induced changes in
448 organization, protein profile and function of photosynthetic machinery in *Chlamydomonas*
449 *reinhardtii*. J. Photochem. Photobiol. B Biol. 152, 367–376.
450 https://doi.org/10.1016/j.jphotobiol.2015.08.025
451 Navarro, E., Piccapietra, F., Wagner, B., Marconi, F., Kaegi, R., Odzak, N., Sigg, L., Behra, R.,
452 2008. Toxicity of Silver Nanoparticles to *Chlamydomonas reinhardtii*.
453 Nikonenko, N.A., Buslov, D.K., Sushko, N.I., Zhbankov, R.G., 2000. Investigation of stretching
454 vibrations of glycosidic linkages in disaccharides and polysaccharides with use of IR spectra
455 deconvolution. Biopolym. - Biospectroscopy Sect. 57, 257–262. https://doi.org/10.1002/1097-
456 0282(2000)57:4<257::AID-BIP7>3.0.CO;2-3
457 Nolte, T.M., Hartmann, N.B., Kleijn, J.M., Garnæs, J., van de Meent, D., Jan Hendriks, A., Baun,
458 A., 2016. The toxicity of plastic nanoparticles to green algae as influenced by surface
459 modification, medium hardness and cellular adsorption. Aquat. Toxicol. 183, 11–20.
460 https://doi.org/10.1016/j.aquatox.2016.12.005
461 Pal, D., Khozin-Goldberg, I., Cohen, Z., Boussiba, S., 2011. The effect of light, salinity, and
462 nitrogen availability on lipid production by Nannochloropsis sp. Appl. Microbiol. Biotechnol.

90, 1429–1441. https://doi.org/10.1007/s00253-011-3170-1

Palmucci, M., Ratti, S., Giordano, M., 2011. Ecological and evolutionary implications of carbon allocation in marine phytoplankton as a function of nitrogen availability: A fourier transform infrared spectroscopy approach. J. Phycol. 47, 313–323. https://doi.org/10.1111/j.1529-8817.2011.00963.x

Park, J.J., Wang, H., Gargouri, M., Deshpande, R.R., Skepper, J.N., Holguin, F.O., Juergens, M.T., Shachar-Hill, Y., Hicks, L.M., Gang, D.R., 2015. The response of *Chlamydomonas reinhardtii* to nitrogen deprivation: A systems biology analysis. Plant J. 81, 611–624. https://doi.org/10.1111/tpj.12747

Patel, S.A., Currie, F., Thakker, N., Goodacre, R., 2008. Spatial metabolic fingerprinting using FT-IR spectroscopy: Investigating abiotic stresses on *Micrasterias hardyi*. Analyst 133, 1707–1713. https://doi.org/10.1039/b809441a

Pfaffl, M.W., Tichopad, A., Prgomet, C., Neuvians, T.P., 2004. Determination of stable housekeeping genes, differentially regulated target genes and sample integrity: BestKeeper – Excel-based tool using pair-wise correlations. Biotechnol. Lett. 26, 509–515. https://doi.org/10.1016/j.ejor.2016.09.013

Puzanskiy, R., Romanyuk, D., Shishova, M., 2018. Coordinated alterations in gene expression and metabolomic profiles of *Chlamydomonas reinhardtii* during batch autotrophic culturing. Biol. Commun. 63, 87–99. https://doi.org/10.21638/spbu03.2018.110

Robichaud, C.O., Uyar, A.E., Darby, M.R., Zucker, L.G., Wiesner, M.R., 2009. Estimates of Upper Bounds and Trends in Nano-TiO_2 Production As a Basis for Exposure Assessment. Environ. Sci. Technol. 43, 4227–4233. https://doi.org/10.1021/es8032549

Sack, L., Zeyl, C., Bell, G., Sharbel, T., Reboud, X., Bernhardt, T., Koelewyn, H., 1994. Isolation of four new strains of *Chlamydomonas reinhardtii* (Chlorophyta) from soil samples. J. Phycol. 30, 770–773. https://doi.org/10.1088/1742-6596/194/4/042018

Sadiq, I.M., Dalai, S., Chandrasekaran, N., Mukherjee, A., 2011. Ecotoxicity study of titania (TiO_2)

NPs on two microalgae species: Scenedesmus sp. and Chlorella sp. Ecotoxicol. Environ. Saf. 74, 1180–1187. https://doi.org/10.1016/j.ecoenv.2011.03.006

Schmollinger, S., Mühlhaus, T., Boyle, N.R., Blaby, I.K., Casero, D., Mettler, T., Moseley, J.L., Kropat, J., Sommer, F., Strenkert, D., Hemme, D., Pellegrini, M., Grossman, A.R., Stitt, M., Schroda, M., Merchant, S.S., 2014. Nitrogen-sparing mechanisms in Chlamydomonas affect the transcriptome, the proteome, and photosynthetic metabolism. Plant Cell 26, 1410–1435. https://doi.org/10.1105/tpc.113.122523

Sjollema, S.B., Redondo-Hasselerharm, P., Leslie, H.A., Kraak, M.H.S., Vethaak, A.D., 2016. Do plastic particles affect microalgal photosynthesis and growth? Aquat. Toxicol. 170, 259–261. https://doi.org/10.1016/j.aquatox.2015.12.002

Stehfest, K., Toepel, J., Wilhelm, C., 2005. The application of micro-FTIR spectroscopy to analyze nutrient stress-related changes in biomass composition of phytoplankton algae. Plant Physiol. Biochem. 43, 717–726. https://doi.org/10.1016/j.plaphy.2005.07.001

Stone, V., Nowack, B., Baun, A., van den Brink, N., von der Kammer, F., Dusinska, M., Handy, R., Hankin, S., Hassellöv, M., Joner, E., Fernandes, T.F., 2010. Nanomaterials for environmental studies: Classification, reference material issues, and strategies for physico-chemical characterisation. Sci. Total Environ. 408, 1745–1754. https://doi.org/10.1016/j.scitotenv.2009.10.035

Szivák, I., Behra, R., Sigg, L., 2009. Metal-induced reactive oxygen species production in *Chlamydomonas reinhardtii* (chlorophyceae). J. Phycol. 45, 427–435. https://doi.org/10.1111/j.1529-8817.2009.00663.x

Tang, Y., Xin, H., Malkoske, T., Yin, D., 2017. The toxicity of Nanoparticles to Algae, in: Bioactivity of Engineered Nanoparticles. Springer, pp. 1–20. https://doi.org/10.1007/978-981-10-5864-6

Ter Halle, A., Jeanneau, L., Martignac, M., Jardé, E., Pedrono, B., Brach, L., Gigault, J., 2017. Nanoplastic in the North Atlantic Subtropical Gyre. Environ. Sci. Technol. 51, 13689–13697.

https://doi.org/10.1021/acs.est.7b03667

Umezawa, I., Komiyama, K., 1985. Acidic polysaccharide CH-1 isolated from *Chlorella pyrenoidosa* and the use thereof. U.S. Pat. 5976719. https://doi.org/US006040467A

Valledor, L., Furuhashi, T., Hanak, A.M., Weckwerth, W., 2013. Systemic cold stress adaptation of *Chlamydomonas reinhardtii*. Mol. Cell. Proteomics 12, 2032–2047. https://doi.org/10.1074/mcp.M112.026765

von Moos, N., Slaveykova, V.I., 2014. Oxidative stress induced by inorganic nanoparticles in bacteria and aquatic microalgae--state of the art and knowledge gaps. Nanotoxicology 8, 605–630. https://doi.org/10.3109/17435390.2013.809810

Wang, C., Peng, X., Wang, J., Lei, A., Li, H., Hu, Z., 2016. A β-carotene ketolase gene (bkt1) promoter regulated by sodium acetate and light in a model green microalga *Chlamydomonas reinhardtii*. Algal Res. 20, 61–69. https://doi.org/10.1016/j.algal.2016.09.020

Wiercigroch, E., Szafraniec, E., Czamara, K., Pacia, M.Z., Majzner, K., Kochan, K., Kaczor, A., Baranska, M., Malek, K., 2017. Raman and infrared spectroscopy of carbohydrates: A review. Spectrochim. Acta - Part A Mol. Biomol. Spectrosc. 185, 317–335. https://doi.org/10.1016/j.saa.2017.05.045

Zarrinmehr, M.J., Farhadian, O., Heyrati, F.P., Keramat, J., Koutra, E., Kornaros, M., Daneshvar, E., 2019. Effect of nitrogen concentration on the growth rate and biochemical composition of the microalga, *Isochrysis galbana*. Egypt. J. Aquat. Res. 46, 153–158. https://doi.org/10.1016/j.ejar.2019.11.003

1. Introduction

Essentials Oils (EO) extracts from plants have been the focus of numerous studies due to their potential in the pharmaceutical and food industries. Several works and patents have been developed specifically for the application of EO and their components into the food sector (Ribeiro-Santos et al., 2017; Llana-Ruiz- Cabello et al., 2015; Maisanaba et al., 2017). Globally, their relatively safe status, properties and acceptance by consumers which demand natural compounds to replace synthetic ones have piqued the interest of industries and consumers (Sacchetti et al., 2005; Benkeblia and Lanzotti, 2007; Debiagi et al., 2014). Among those beneficial plants, *Allium* sp. is a genus well-known for its antimicrobial, antiviral, antiprotozoal, antifungal or antioxidant properties (among others). These properties are mainly due to their content of organosulfur compounds (OSC), which are secondary phytochemical metabolites, biosynthesized for defensive purposes against biotic and abiotic stressors. They are mainly formed for the action of the enzyme alliin (stored in vacuoles) on cytoplasmic compounds like alk(en)yl cysteine sulfoxides (ACOs) once the vegetable tissue is hurt (Putnik et al., 2019) (Fig. 1). Otherwise, these compounds are not available in intact cells as they are toxic for the plant (Ramirez et al., 2017).

One of the main components of *Allium* essential oil is propyl-propane-thiosulfonate (PTSO), that corresponds to the molecular formula $C_6H_{14}O_2S_2$ (Fig. 1). This compound has been stabilized and characterized by DMC Research Center SLU (Granada, Spain) to be used for different applications, taking advantage of its beneficial properties. Thus, this product has been reported to show mainly antioxidant and antimicrobial activities, being able to inhibit the growth of Gram (–) and Gram (+) bacteria as well as molds and yeast (Peinado et al., 2012, 2013; Llana-Ruiz-Cabello et al., 2015). Its antibacterial activity *in vitro* in humans has also been demonstrated (Sorlozano-Puerto et al., 2018).

Proallium AP®, a commercial *Allium* sp. extract with a 14.5% PTSO content, has been proposed as a biopreservative in active food packaging for human food commodities mainly due to its antioxidant and antimicrobial activity (Llana-Ruiz-Cabello et al., 2018). The packaging material used in these systems can incorporate components intended to be released into the food from the package, allowing foods to arrive at the consumers with their original or enhanced organoleptic properties, with longer shelf-life and safety (Ribeiro-Santos et al., 2017). Previously, another study carried out by Seydim & Sarikus, (2006) tested the antimicrobial activity of garlic EO in combination with oregano EO in films made with whey protein isolate, and showed antimicrobial activity in a concentration of 4% (w/v). But the incorporation of garlic EO and their components in active food packaging can result in a higher human exposure and consequently, more research is needed to stablish the safety concentration. An additional proposed application for PTSO is as sensory additive in animal nutrition, improving the palatability of feed, and also as a zootechnical additive, being an alternative to the use of antibiotics (Peinado et al., 2012), contributing to reduce resistance generated by their excessive use in livestock. Since the ban in the European Union (EU) of the use of antibiotics as growth promoters, the search for new alternative products that ensure similar production levels and food security without generating unwanted effects, including human resistances, has been fostered, being additives of natural origin a good alternative. The regulation (EC) No 1831/2003 of the European Parliament and of the Council of 22 September 2003 sets the parameters of use of the additives used in animal nutrition. Recent studies have shown that some feed additives can help animals to maintain good physiological conditions and improve animal welfare. This has led to an amendment in the abovementioned regulation on 12th June 2019, establishing new functional groups of feed additives to improve

physiological condition of animals. In this regard, other properties demonstrating the potential use of PTSO in animal nutrition sector are the anti-methanogenic effect described during the fermentation process in rumen (Martínez-Fernández et al. 2013) and the immunomodulatory and anti-inflammatory properties (Vezza et al., 2019).

However, the successful development of any application of this compound must be accompanied by an extensive toxicological evaluation, that guarantees its safety for the final consumers, both humans and livestock.

In this regard, the toxicological profile of PTSO has been investigated by cytotoxicity assays in human cell lines (Llana-Ruiz-Cabello et al., 2015) as well as its genotoxicity and mutagenicity *in vitro* (Mellado-García et al., 2015) and genotoxicity *in vivo* (Mellado-Garcia et al., 2016b). Furthermore, its acute toxicity *in vivo* has been also evaluated (Llana-Ruiz-Cabello et al., 2015). Notwithstanding, safe doses of use have been not yet established for PTSO. Thus, a repeated dose 90-days oral toxicity study in rodents of PTSO would be necessary to clearly characterize its toxicity, being also a requirement in the authorization application processes of the European Food Safety Authority (EFSA, 2012; 2016a; 2016b; 2017).

The aim of the present study is, therefore, to further explore the toxicity potential of PTSO and, for the first time, to conduct a subchronic dietary toxicity assay of PTSO in rats following internationally recognized test guidelines (Organisation for Economic Co-operation and Development, OECD 408, 2018). Considering these facts, in the present study several parameters have been evaluated, including body weight changes, food and water consumption, feed conversion efficiency, organ weight ratios and biochemistry and hematology parameters. In addition the histopathology of various tissues has been also studied. The results from the complete assessment of this

subchronic study would allow to get an estimation of a non-observed-adverse-effect-level (NOAEL) of exposure to establish safety conditions for human exposure to PTSO.

2. Materials and Methods

2.1. Test item and doses preparation

PTSO was supplied by DMC RC SLU (Granada, Spain) with a 96% of purity. Commercial powder neutral gelatin from pork protein (Jesus Navarro S.A., Alicante, Spain) was employed as the vehicle for the test substance in all groups including the controls.

For the 90-days study, the doses were prepared daily for each animal during the 13 weeks, and on Fridays they were also prepared for the weekend. The dose was mixed in 3 mL of liquid gelatin. The volumes of PTSO (µL) to add to the gelatin depended on the dose selected for each group, and the gelatin could solidify at 4 ºC overnight. Homogeneity of the dietary dose formulations and their stability were confirmed to be at least 5 days.

2.2. Animals conditions and husbandry services

The rats were supplied by Charles River laboratories S.L. (Kings, NY, USA), 40 males and 40 females of Sprague-Dawley strain. They were approximately 7 weeks old and were stabilized for an acclimatization period of 7 days during which they were examined by a veterinary surgeon. When the first week of dosage began the rats body weight mean was 320 g ± 11.3 for males and 227 ± 11.9 for females.

Animals were individually housed in cages type 3H with Souralit 29/12 plus (souralit S.L., Gerona, Spain) aspen wood bedding and food completely available without restriction using standard dry pellet diet for rodents Scientific (Panlab, S.L.U., Cornella de Llobregat, Barcelona, Spain). They were kept in a room with controlled conditions of hygiene behind a barrier system, a range of temperature of 21±2ºC, with a 10-15 air changes per hour, and a relative humidity between 30-70% under 12 h light/dark cycle. Each cage contained an information card which contained study code (19-CAM-11-animal number), sex, dose, group, and individual animal identification. Community tap water (EMACSA, Cordoba Water company, Córdoba, Spain), filtered and autoclaved was available *ad libitum.*

2.3. Study design

The maximum tolerable dose (MTD) for PTSO in rats orally exposed to PTSO (gavage) was previously set at 55 mg/kg by Llana-Ruiz-Cabello et al., (2015) following the OECD 425 (2008) test guideline (oral toxicity study: Up and Down procedure), and it was used as a reference to establish the test doses. Accordingly, this dose was selected as the highest one to be tested, and also descending doses using a 2-fold interval factor according to the guideline OECD 408 (2018) recommendations: 14, 28, 55 mg/kg/day. Rats (10/sex/group) were orally administered the selected doses and the control group received only the vehicle (pork gelatine).

This study was performed at the Central Service of Experimental Animals from the University of Cordoba (SAE, Cordoba, Spain) in which all animals received human care in accordance with the guidelines for the protection of animals used for the science

purposes (Directive, 2010/63 EU, Decision, 2012/707/UE, and RD 53/2013). All procedures have been approved by the Ethical Animal Experimentation Committee of the University of Córdoba and by the Junta de Andalucía (project nº 20/10/2015-348).

2.4. Clinical observations

Each animal was observed twice daily for morbidity and mortality and once daily for clinical signs, such as changes in skin, fur, eyes or mucous membranes; secretions; changes in gait, posture, or handling response; abnormal, clonic, or tonic movements, and stereotypes or bizarre behavior. Ophthalmic examinations were performed on all animals before initiating the study and in the control and in the highest dose group at the end of treatment.

2.5. Body weight, food and water consumption

These three parameters were checked weekly in order to avoid stress. The mean body weight per group and sex were calculated weekly and prior to necropsy from individual animals' data, as well as the food and water consumption. The total food consumed per cage was recorded and the weekly mean intake per rat was calculated. The feed conversion efficiency (FCE) ratio was determined according to Escobar et al., (2015) by the ratio of food intake (g)/ weight gained (g).

2.6. Hematology and Biochemistry

Blood samples were extracted from the heart by an intracardiac injection under light isofluorane anesthesia at week 13. Then, the hematological parameters were

estimated on an automatic hematology analyzer Cell-Dyn 3700 (Abbot, GMI, MI, USA): red blood cell count (RBC), hemoglobin (HGB), hematocrit (HCT), mean corpuscular volume (MCV), mean corpuscular hematoglobin (MCH), mean corpuscular hematoglobin concentration (MCHC), blood platelet count (PLT), red cell volume distribution (RDW), prothrombin time (PT), cefaline time (CT), white blood cell count (WBC), Neutrophils (NE), Lymphocites (LY), Monocytes (MO), Eosinophils (EO) and Basophils (BA).

An automatic chemistry analyzer Cobas 6000 (Roche Diagnostics, IN, USA) was used to determinate the following standard biochemistry parameters: glucose (GLUC), blood urea nitrogen (UREA), creatinine (CREAT), bile acids (BILI-T), total cholesterol (CHOL), triglycerides (TRIGL), aspartate aminotransferase (AST), alanine aminotransferase (ALT), alkaline phosphatase (ALKP), albumin (ALB), total protein (TOT PROT), sodium (Na^+), potassium (K^+) and Calcium (Ca^{2+}) ions.

2.7. Necropsy and Organ weight

The animals were fasted for 18 h before the sacrifice and profoundly anaesthetized with isofluorane, then exsanguinated by intracardiac injection. All rats were given a complete pathology examination through the necropsy. The following organs were collected from animals at necropsy and weighed wet immediately after dissection: brain, liver, heart, spleen, kidneys, thymus, adrenal glands, uterus with cervix and ovaries (females) and testes and epididymis (males). In addition, tissue samples of the following organs were taken from the control and the highest dose (55 mg/kg/day) group for histopathological examination under light microscopy: liver, kidney, spleen, heart, brain, pituitary, stomach, intestine, lung, testicle/ovary and

skeletal muscle. Samples were fixed in 10% formalin for 24h at 4ºC, and then immediately dehydrated in graded series of ethanol, deep in xylol and embedded in paraffin wax using an automatic processor. Sections of 3-5 µm were mounted. After they had been deparaffinized, the sections were rehydrated, stained with hematoxylin and eosin, and mounted with Cristal/Mount (Paraplat, Oxford Labware, St. Louis, MO.).

2.8. Statistical analysis

All statistical analysis were carried out using Graph-Pad Instant software (GraphPadSoftware Inc., La Jolla, USA). Continuous variables, such as body weight, body weight gain, food and water consumption, hematology, clinical chemistry, and organ weight, were summarized using standard measures of central tendency and dispersion, mean and standard deviation (ST. DEV.), and were reported by sex and dosage. One-way analysis of variance (ANOVA) was carried out to test differences in continuous variables. Normality assumption was tested using Kolmogorov-Smirnov's test. If non-normality, comparison was performed with Kruskal Wallis test. In case of significant differences, multiple comparisons were performed using Tukey-Kramer/Dunn's Multiple Comparisons Tests. Differences were considered significant from $P < 0.05$.

3. Results

3.1. Survival and clinical observations

No unscheduled deaths occurred during the study. Light clinical signs were observed in some animals. Thus, sporadic alopecia was observed in rats 47, 59 and 62; small wounds in the ear of rat 52 and hematoma in the ear of rat 14 satisfactorily

recovered. These signs were not considered to be related to the test item, and were not biologically significant. Ophthalmologic examination revealed no compound-related lesions in the highest dose group of animals. No other clinical observations were noted.

3.2. Body weight, body weight gain, food and water consumption, feed consumption efficiency

Body weight increased along the study period following a usual pattern for this species. The test item did not induce any statistically significant alteration in this parameter (Fig. 2). Similarly, the body weight gain increased along the 13 weeks, with no differences between the control and the exposed groups in both sexes (Fig. 3).

Food and water consumption per week did not show significant differences between control and treated groups, male and female, throughout the duration of the study, following the usual pattern (data not shown). The feed consumption efficiency also did not reveal any remarkable change for animals (Table 1). Thus, the test item did not have a negative impact on these parameters.

3.3. Hematology and blood chemistry

Hematology parameters evaluated in rats exposed to PTSO are provided in Table 2. All variables considered remained unaltered in males. However, in females HCT (%) showed a significant increase ($p<0.5$) in groups 2 and 3 (14 and 28 mg/Kg/d, respectively) in comparison to group 4 (50 mg/Kg/d), and also the MCH (pg) experienced a significant decrease ($p<0.5$) in group 2 (14 mg/Kg/d) in comparison to group 3 (28 mg/Kg/d).

The differential White blood cells count did not show any change in any of the exposed groups and neither in males nor females (Table 3).

Table 4 includes the clinical biochemistry values obtained for the parameters analyzed after the oral subchronic exposure of rats to PTSO. Most of them were not modified by the treatment. Only in males, a significant ($p<0.01$) decrease of Chol (mg/dL) values was observed in the highest dose group (55 mg/Kg/day), and also a significant increase ($p<0.5$) of TRIGL (mg/dL) in the lowest dose group (14 mg/Kg/day), in comparison to the control group.

In general, as the significant changes observed were minimal, sporadic, not present in all dose groups, neither in both sexes, they were considered incidental and not indicative of toxicity.

3.4. Necropsy, organ weights and histopathology

No gross pathologies were observed during the necropsy in any of the experimental animals. Also, organ weights were not altered by the treatment and only the mean heart weight of males of group 3 (28 mg/Kg/day) showed a slight but significant ($p<0.5$) decrease in comparison to the control group (Table 5). This was considered to be not related to the test item. Moreover, no significant changes were recorded in the organ weight/body weight ratio (Table 6) neither in the organ weight/brain weight ratio (Table 7).

Regarding to the histopathological study performed, tissues of the rats, both male and female, exposed to the highest dose, did not revealed alterations in comparison to the control group in any of the organs examined by light microscopy (Fig. 4).

4. Discussion

The repeated dose 90-days oral toxicity study in rodents provides information on the possible health hazards likely to arise from repeated exposure over a prolonged period of time covering post-weaning maturation and growth into adulthood of the test animals. The study provides, among others, information on the major toxic effects, identification of target organs and also can provide an estimate of a non-observed-adverse-effect level (NOAEL) of exposure which can be used in selecting dose levels for chronic studies and for establishing safety criteria for human exposure (OECD 408, 2018). Moreover, an oral 90-days subchronic toxicity assay is usually included among the basic set of toxicity tests required in the evaluation of chemical substances with potential applications in the agri-food sector before their authorization. This is the case for example of food (EFSA, 2012a) and feed additives (EFSA, 2017), migrating food contact materials (EFSA, 2016a), or novel food (2016b). All this highlights the relevance of the study performed with PTSO, as this compound has shown beneficial properties with different potential applications previously described.

The general absence of toxic effects observed after the treatment allows to estimate that the NOAEL for PTSO is ≥ 55 mg/Kg/day. Considering a safety factor of 100 usually applied in food additives to derive human safety values from animal data (EFSA, 2012b), a dose of 0.55 mg/Kg/day could be suggested as a safe human exposure (~ 38,5 mg/day for a 70 kg b.w. person). However, this value is underestimated taking into account that a NOAEL could not be established from the assay performed and could be higher than 55 mg/Kg/day.

The results obtained in the present study complete the information available in relation to the toxicity profile of PTSO. Thus, Llana-Ruiz-Cabello et al. (2015)

performed an acute oral toxicity test (Up-and-Down Procedure) following the OECD 425 guideline (2008) and 55 mg/Kg b.w. was established as the maximum tolerated dose (MTD) in rats. However, in that case the exposure was by gavage whereas in the present study it was with the diet, a more realistic human exposure scenario.

Mellado-García et al. (2015) performed a thorough *in vitro* genotoxicity assessment of PTSO including 4 different tests, among them the Ames test and the Micronucleous (MN) assay. This is the basic battery indicated by EFSA (2012) as they cover the three genetic endpoints required: gene mutations and both structural and numerical chromosome aberrations. They also performed the Mouse Lymphoma assay (MLA) and the Comet assay. They concluded that PTSO was not mutagenic in the Ames test, but it was mutagenic in the MLA assay after 24 h of treatment. The parent compound did not induce MN on mammalian cells; however, its metabolites induced positive results. Due to inconclusive results, a follow-up of positive *in vitro* results by *in vivo* testing was performed. The genotoxicity of PTSO in rats following an oral administration of 5.5, 17.4 and 55 mg/kg was evaluated by a combined *in vivo* comet assay and MN test (Mellado-Garcia et al., 2016a) and the results revealed no genotoxicity.

All these results suggest a safety profile of PTSO for food applications at the doses assayed, but in a risk assessment frame it is well known that risk depends not only on the hazard but also in the human exposure level. In this regard, the level of PTSO to use, and therefore the potential exposure, will depend on the specific application considered. For instance, in the active packaging of lettuce, Llana-Ruiz-Cabello et al. (2015) estimated that in the worst-case scenario a human could ingest 6.87 mg PTSO, this means only a 18% of the dose calculated as safe in the present study.

The results obtained agree with those of Mellado et al. (2016b) who evaluated the safety of Proallium AP®, an *Allium*-based commercial product in a 90-days feeding study with rats. PTSO is actually the major organosulfur compound present in Proallium AP® (14.5%). Similarly, neither clinical signs nor any other changes on general, biochemical, hematological or histopathological parameters were detected, and the authors derived a NOAEL higher than 400 mg/Kg/day at the conditions assayed. Both studies show a good correlation as in the present study the test item had a 7-fold higher content of PTSO than Proallium® AP (100 versus 14.5%) and the NOAEL derived for Proallium was 7-fold higher. This suggests that PTSO has an important role on the toxicity of *Allium* extracts. Actually, a MTD of 55 mg/kg in rats for PTSO has been established as previously indicated. And higher doses tested according to the OECD 425 guideline (2000 mg/kg and 175 mg/kg) resulted in the death of the animal and evident hepatotoxicity. On the contrary, a single dose of 55 mg/kg did not induce remarkable damage (Llana-Ruiz-Cabello et al, 2015). Mellado-García et al. (2016a) observed that in rats treated with 55 mg/kg (3 doses at 0, 24 and 45h and euthanized at 48h) an increase in the glycogen storage was noticeable in the liver and also a slight degenerative process in the chief cells of the stomach.

In this regard, at the dose levels assayed, histopathological lesions were absent. This could be explained by the exposure way employed in this study, using gelatin as vehicle and with the feed. In the previous trials, oral gavage with a stomach tube after a fasting period was used following the recommendations of the corresponding OCDE guidelines. The bolus could have a more deleterious effect on the gastrointestinal system as there is a direct contact.

Differences in toxicity between PTSO and Proallium AP® could be explained as the toxicity shown by components of an essential oil can be modulated by the other

constituents by synergistic/antagonistic phenomena (Escobar et al., 2015; Pavlidou et al., 2004). The interest of PTSO in comparison to Proallium® is based on its different chemical properties (higher hydrophilia) and in its higher efficiency on its antioxidant and antimicrobial properties.

Other authors have shown the potential toxicity of aqueous extracts of different medicinal plants, including *Allium sativum*, in Wistar rats. Thus, Sulaiman et al. (2014) administered orally to the animals 10 mg/kg of *A. sativum* extract for 30 days and observed alteration in the activities of marker enzymes: AST increased in liver, kidney and heart, ALT in serum and liver, and ALP activity was reduced in serum, heart, kidney and liver. They concluded that caution was required in using unrefined extracts of these herbs in traditional settings.

There are scarce *in vivo* toxicity data regarding other OSC. Thus, Guyonnet et al. (2000) demonstrated the effects of some of them (DAS, DADS, dipropylsulfiide (DPS) and dipropyl disulfide (DPDS)) on the activation of several mutagens in male Wistar rats exposed to 1 mmol/kg by gavage for 4 days. They explained the results based on the induction of cytochrome (CYP) and phase II enzymes activities. This effect, the alteration of CYP activity, was pointed out by other authors as well (Davenport and Wargovich, 2005). Moreover, they observed hepatotoxicity induced by DAS (bile duct obstruction, hyperproliferation and focal points of necrosis) in rats gavaged daily with 200 mg/kg for 1, 4, or 8 weeks. On the contrary, 8 weeks of exposure to lower doses (50 and 100 mg/kg) did not induced liver histophatological damage. This suggest that liver could be the target organ of OSC as both, DAS (Davenport and Wargovich, 2005) and PTSO (Llana-Ruiz-Cabello et al, 2015), have shown liver toxicity when a threshold dose is exceeded. Also, Wu et al. (2001) exposed rats orally to garlic oil (GO, 200 mg/Kg) and 3 allyl compounds, DAS (20 and 80 mg/kg), DADS (80 mg/kg), and diallyl

trisulfide (DATS, 70 mg/kg) 3 times a week for 6 weeks and examined the antioxidation system in rat livers and red blood cells. They found that GO, DADS and DATS significantly induced the glutathione content (GSH) in blood cells but neither GO nor any of its OSC affected the GSH-related antioxidant enzymes. Hepatic GSH was not influenced by garlic components. But DADS and DATS significantly increased the activity of GSH-reductase and GSH-transferase and decreased GSH peroxidase. In the present study the hematological parameters were not influenced by the PTSO exposure and scarce scientific data dealing with PSTO are available to compare.

5. Conclusions

In conclusion, the results obtained confirm the already reported safety profile of PTSO for some food applications at the conditions considered. Thus, PTSO did not promote toxic effects as seen from body weight changes, food and water consumption, feed conversion efficiency, biochemical and blood parameters as well as organ toxicity and histological examinations of main organs that could eventually be affected by its subchronic administration (90 days). NOAEL was estimated to be ≥ 55 mg/Kg/day.

Conflict of Interest

The authors declare that there are no conflicts of interest.

Acknowledgements

The authors would like to acknowledge the Spanish Ministerio de Ciencia e Innovación (Project RTC-2017-6199-2), and to the Junta de Andalucía (Project AT 2017-5323) for its financial support.

References

Benkeblia, N., Lanzotti, V. (2007). Allium thiosulfinates: chemistry, biological properties and their potential utilization in food preservation. Food 1, 193–201.

Davenport, D.M., Wargovich, M.J. (2005). Modulation of cytochrome P450 enzymes by organosulfur compounds from garlic. Food Chem. Toxicol. 43, 1753-1762. doi: 10.1016/j.fct.2005.05.018.

Debiagi, F., Kobayashi R.K.T., Nakazato, G., Panagio, L.A., Mali, S. (2014). Biodegradable active packaging based on cassava bagasse, polyvinylalcohol and essential oils. Ind. Crop. Prod. 52, 664-670. doi.org/10.1016/j.indcrop.2013.11.032

European Food Safety Authority, 2008. Guidance Document on the Submission of a Dossier on a Substance to Be Used in Food Contact Materials for Evaluation by EFSA by the Panel on Food Additives, Flavourings, Processing Aids and Materials in Contact with Food (AFC)

EFSA Panel on Food Additives and Nutrient Sources added to Food (ANS); Guidance for submission for food additive evaluations. EFSA Journal 2012a;10(7):2760. [60 pp.] doi:10.2903/j.efsa.2012.2760. Available online: www.efsa.europa.eu/efsajournal.

EFSA Scientific Committee; Guidance on selected default values to be used by the EFSA Scientific Committee, Scientific Panels and Units in the absence of actual measured data. EFSA Journal 2012b;10(3):2579. [32 pp.] doi:10.2903/j.efsa.2012.2579.

EFSA CEF Panel (EFSA Panel on Food Contact Materials, Enzymes, Flavourings and Processing Aids), 2016a. Scientific opinion on recent developments in the risk assessment of chemicals in food and their potential impact on the safety assessment of substances used in food contact materials. EFSA Journal 2016;14(1):4357, 28 pp. doi:10.2903/j.efsa.2016.4357.

EFSA NDA Panel (EFSA Panel on Dietetic Products, Nutrition and Allergies), Turck D, Bresson J-L, Burlingame B, Dean T, Fairweather-Tait S, Heinonen M, Hirsch-Ernst KI, Mangelsdorf I, McArdle H, Naska A, Neuhauser-Berthold M, Nowicka G, Pentieva K, Sanz Y, Siani A, € Sjodin A, Stern M, Tom € e D, Vinceti M, Willatts P, Engel K-H, Marchelli R, P oting A, Poulsen M, € Salminen S, Schlatter J, Arcella D, Gelbmann W, de Sesmaisons-Lecarre A, Verhagen H and van Loveren H, 2016b. Guidance on the preparation and presentation of an application for authorisation of a novel food in the context of Regulation (EU) 2015/2283. EFSA Journal 2016;14(11):4594, 24 pp. doi:10.2903/j.efsa.2016.4594.

EFSA FEEDAP Panel (EFSA Panel on Products or Substances used in Animal Feed), Rychen G, Aquilina G, Azimonti G, Bampidis V, Bastos ML, Bories G, Chesson A, Cocconcelli PS, Flachowsky G, Gropp J, Kolar B, Kouba M, Lopez-Alonso M, L opez Puente S, Mantovani A, Mayo B, Ramos F, Saarela M, Villa RE, Wallace RJ, Wester P, Anguita M, Dujardin B, Galobart J and Innocenti ML, 2017. Guidance on the assessment of the safety of feed additives for the consumer. EFSA Journal 2017;15(10):5022, 17 pp. https://doi.org/10.2903/j.efsa.2017.5022

Escobar, F.M., Sabini, M.C., Cariddi, L.N., Sabini, L.I., Manas, F., Cristofolini, A., Bagnis, G., Gallucci, M.N., Cavaglieri, L.R. (2015). Safety assessment of essential oil from *Minthostachys verticillata (*Griseb.) Epling (peperina): 90-days oral

subchronic toxicity study in rats. Regul. Toxicol. Pharm. 71, 1-7. doi: 10.1016/j.yrtph.2014.11.001.

Guyonnet, D., Belloir, C., Suschetet, M., Siess, M.H., Le Bon, A.M. (2000). Liver subcelular fractions from rats treated by organosulfur compounds from Allium modulate mutagen activation. Mutat. Res. 466, 17-26. doi.org/10.1016/S1383-5718(99)00234-X

Llana-Ruiz-Cabello, M., Pichardo S., Maisanaba S., Puerto M., Prieto A.I., Gutiérrez-Praena, D., Jos, A., Cameán, A.M. (2015). *In vitro* toxicological evaluation of compounds from essential oils used in active Food packaging: a review. Food Chem. Toxicol., 81, 9-27. doi: 10.1016/j.fct.2015.03.030.

Llana-Ruiz-Cabello, M., Gutiérrez-Praena, D., Puerto, M., Pichardo, S., Moreno, F.J., Baños, A., Nuñez, C., Guillamón, E., Cameán, A.M. (2015). Acute toxicological studies of the main organosulfur compound derived from Allium sp. intended to be used in active food packaging. Food Chem. Toxicol. 82, 1-11. doi: 10.1016/j.fct.2015.04.027.

Llana-Ruiz-Cabello, M., Pichardo, S., Bermudez, J.M., Baños, A., Ariza, J.J., Guillamón, E., Aucejo, S., Cameán, A.M. (2018). Characterisation and antimicrobial activity of active polypropylene films containing oregano essential oil and Allium extract to be used in packaging for meat products. Food. Addit. Contam. Part. A. Chem. Anal. Control. Expo. Risk. Assess. 35(4):782-791. doi: 10.1080/19440049.2017.1422282.

Maisanaba, S., Llana-Ruiz-Cabello, M., Gutiérrez-Praena, D., Pichardo, S., Puerto, M., Prieto, A.I., Jos, Á., Cameán A.M. (2017). New advances in active packaging

incorporated with essential oils or their main components for food preservation. Food. Rev. International 33, 447-515. .doi. 10.1080/87559129.2016.1175010

Mellado-Garcia, P., Maisanaba, S., Puerto, M., Llana-Ruiz-Cabello, M., Prieto, A.I., Marcos, R., Pichardo, S., Cameán, A.M. (2015). Genotoxicity assessment of propyl thiosulfinate oxide, an organosulfur compound from *Allium* extract, intended to food active packaging. Food Chem. Toxicol. 86, 365-373. doi.org/10.1016/j.fct.2015.11.011

Mellado-Garcia, P., Puerto, M., Prieto, A.I., Pichardo, S., Martín-Cameán, A., Moyano, R., Blanco, A., Cameán, A.M. (2016a). Genotoxicity of a thiosulfonate compound derived from *Allium* sp. intended to be used in active food packaging: *In vivo* comet assay and micronucleus test. Mutat. Res. 800-801, 1-11. doi.org/10.1016/j.mrgentox.2016.03.001

Mellado-Garcia, P., Puerto, M., Pichardo, S., Llana-Ruiz-Cabello, M., Moyano, R., Blanco, A., Jos, A., Cameán, A.M. (2016b). Toxicological evaluation of an *Allium*-based commercial product in a 90-day feeding study in Sprague–Dawley rats. Food Chem. Toxicol. 90, 18-29. doi.org/10.1016/j.fct.2016.01.019

Pavlidou, V., Karpouhtsis, I., Franzios, G., Zambetaki, A., Scouras, Z., Mavragani-Tsipidou, P. (2004). Insecticidal and genotoxic effects of essential oils of Greek sage, *Salvia fruticosa*, and mint, *Mentha pulegium*, on *Drosophila melanogaster* and *Bactrocera oleae* (Diptera: Tepritidae). J. Agr. Urban. Entomol. 21, 39-49.

Peinado, M.J., Ruiz, R., Echávarri, A., Rubio, L.A. (2012). Garlic derivative PTS-O is effective against broiler pathogens *in vivo*. Poult. Sci. 91, 2148–2157. doi.org/10.3382/ps.2012-02280

Peinado, M.J., Ruiz, R., Echávarri, A., Aranda-Olmedo, I., Rubio, L.A. (2013). Garlic derivative PTS-O modulates intestinal microbiota composition and improves digestibility in growing broiler chickens. Anim. Feed Sci. Technol. 181, 87–92. doi.org/10.3382/ps.2012-02280

Putnik, P., Gabrić, D., Roohinejad, S., Barba, F.J., Granato, D., Mallikarjunan, K., Lorenzo J.M., Bursać Kovačević, D. (2019). An overview of organosulfur compounds from *Allium* spp.: From processing and preservation to evaluation of their bioavailability, antimicrobial, and anti-inflammatory properties. Food Chem. 276, 680–69. doi.org/10.1016/j.foodchem.2018.10.068.

Ribeiro-santos, R., Andrate, M., Ramos de Melo, M., Sanches-Silva, A. (2017). Use of essential oils in active food packaging: Recent and future trends. Trends. Food. Sci. Technol. 61, 132-140. https://doi.org/10.1016/j.tifs.2016.11.021

Ramirez, D. A., Locatelli, D. A., González, R. E., Cavagnaro, P. F., & Camargo, A. B. (2017). Analytical methods for bioactive sulfur compounds in Allium: An integrated review and future directions. J. Food Compos. Anal. 61, 4–19. https://doi.org/10.1016/j.jfca.2016.09.012.

Sacchetti, G., Maietti, S., Muzzoli, M., Scaglianti, M., Manfredini, S., Radice, M., Bruni, R. (2005). Comparative evaluation of 11 essential oils of different origin as functional antioxidants, antiradicals and antimicrobials in foods. Food. Chem. 91, 621-632. doi.org/10.1016/j.foodchem.2004.06.031

Seydim, A. C., & Sarikus, G. (2006). Antimicrobial activity of whey protein based edible films incorporated with oregano, rosemary and garlic essential oils. Food. Res. Int. 39(5), 639e644. http://dx.doi.org/10.1016/j.foodres.2006.01.013

Solorzano-Puerto, A., Albertuz-Crespo, M., Lopez-Machado, I., Ariza-Romero, J.J., Baños-Arjona, A., Exposito-Ruiz, M., Gutierrez-Fernández, J. (2018). *In Vitro* Antibacterial Activity of Propyl-Propane-Thiosulfinate and Propyl-Propane-Thiosulfonate Derived from *Allium* spp. against Gram-Negative and Gram-Positive Multidrug-Resistant Bacteria Isolated from Human Samples. Biomed. Res. Int. 2018, 1-11. doi: 10.1155/2018/7861207.

Sulaiman, F.A., Kazeem, M.O., Waheed, A.M., Temowo, S.O., Adeyemi, O.S., Nyang, A., Adeyemi, O.S. (2014). Antimicrobial and toxic potential of aqueous extracts of *Allium sativum*, *Hibiscus sabdariffa* and *Zingiber officinale* in Wistar rats. J. Taibah. Univ. Sci. 8, 315-322. doi.org/10.1016/j.jtusci.2014.05.004

Vezza, T., Algieri, F., Garrido-Mesa, J., Utrilla, M.P., Rodríguez-Cabezas, M.E., Baños, A., Guillamón, E., García, F., Rodríguez-Nogales, A., Gálvez, J. (2019). The immunomodulatory properties of propyl-propane thiosulfonate contribute to its intestinal anti-inflammatory effect in experimental colitis. Mol. Nutr. Food Res. 63(5):e1800653. doi: 10.1002/mnfr.201800653.

Wu, C.C., Sheen, L.Y., Chen, H.W., Tsai, S.J., Lii, C.K. (2001). Effects of organosulfur compounds from garlic oil on the antioxidation system in rat liver and red blood cells. Food. Chem. Toxicol. 39, 633-569. doi.org/10.1016/S0278-6915(00)00171-X

Figure captions

Fig. 1. Biochemical pathways and chemical structures of organosulfur compounds. (Alk(en)yl cysteine sulfoxides (ACOs); Propyl-propane-thiosulfonate (PTSO); Propyl-propane-thiosulfinate (PTS)).

Fig. 2. Mean body weights (g) of A) male and B) female rats orally exposed to 0, 14, 28 and 55 mg/kg b.w./day PTSO and control rats for 90 days.

Fig. 3. Mean body weight gain (%) of A) male and B) female rats orally exposed to 0, 14, 28 and 55 mg/kg b.w./day PTSO and control rats for 90 days.

Fig. 4. Histopathological study of liver, kidney, spleen, heart, brain, pituitary, stomach, intestines, lung, testes, and and skeletal muscle of untreated Sprague Dawley rats, control (A), and treated (B) with PTSO (55 mg/Kg/day) for 90 days (bars= 50 µm). In the liver, normal hepatic cords and normal polyhedral hepatocytes with central nucleus and clear cytoplasm are seen in control and exposed animals. In the kidney, the renal parenchyma with normal glomeruli and renal tubules is shown in control rats (A), as well as in rats treated with the highest dose of PTSO (B). Detail of the apparently normal spleen parenchyma in control and treated rats (A, B). In the heart, normal cardiac fibers were observed in all groups (A, B). In the brain, the motions of the cerebral cortex are normal (A, B). Details of the apparently normal pituitary are observed in control and treated rats (A, B). Detail of the stomach with apparently normal mucous and glandular cells in control and treated rats (A, B). Intestinal villi with abundant apparently normal enterocytes are shown in all groups. Detail of the control

bronchial epithelium, without alterations in the bronchi and alveoli in the untreated rats (A) as well as in the rats treated with the highest dose (B). Male rat testes showed normal seminiferous tubules and interstitial space (A) that is maintained in treated male rats (B). The ovaries of the treated and control female rats (A, B) presented normal follicles in all groups. Detail of the normal striated skeletal muscle of the treated and control rats (A, B).

Table captions

Table 1. Effect of 90 days oral exposure to PTSO on body weight and food consumption in rats. Values represent the mean ±SD of 10 rats/sex/group. Differences between control and treated groups for male and female rats were evaluated by Kruskal-Wallis test (K.W.) or by ANOVA test (F values).

Table 2. Hematology parameters of male and female rats fed with 0, 14, 28 and 55 mg/kg b.w./day PTSO for 90-days. Values are mean ± SD for 10 rats/sex/group. The differences between control and treated groups for male and female rats were evaluated by Kruskal-Wallis test (K.W.) or by ANOVA test (F values). The significance levels observed are & in comparison to group 4 (55 mg/Kg/d) when $p<0.05$, and # in comparison to group 3 (28 mg/Kg/d) when $p<0.05$.

Table 3. Differential White blood cells count data of male and female rats fed with 0, 14, 28 and 55 mg/kg b.w./day PTSO for 90-days. Values are mean ± SD for 10 rats/sex/group. The differences between control and treated groups for male and female rats were evaluated by Kruskal-Wallis test (K.W.) or by ANOVA test (F values).

Table 4. Clinical biochemistry of male and female rats fed with 0, 14, 28 and 55 mg/kg b.w./d PTSO for 90-days. Values are mean ± SD for 10 rats/sex/group. The differences between control and treated groups for male and female rats were evaluated by Kruskal-Wallis test (K.W.) or by ANOVA test (F values). The significance levels observed are *$p < 0.05$ and **$p < 0.01$ in comparison to control group values.

Table 5. Absolute organ weight of male and female rats fed with 0, 14, 28 and 55 mg/kg b.w./day PTSO for 90-days. Values are mean ± SD for 10 rats/sex/group. The differences between control and treated groups for male and female rats were evaluated by Kruskal-Wallis test (K.W.) or by ANOVA test (F values). The significance levels observed are *$p < 0.05$ in comparison to control group values.

Table 6. Relative organ weight/body weight of male and female rats fed with 0, 14, 28 and 55 mg/kg b.w./day PTSO for 90-days. Values are mean ± SD for 10 rats/sex/group. The differences between control and treated groups for male and female rats were evaluated by Kruskal-Wallis test (K.W.) or by ANOVA test (F values).

Table 7. Relative organ weight/brain weight of male and female rats fed with 0, 14, 28 and 55 mg/kg b.w./day PTSO for 90-days. Values are mean ± SD for 10 rats/sex/group. The differences between control and treated groups for male and female rats were evaluated by Kruskal-Wallis test (K.W.) or by ANOVA test (F values).

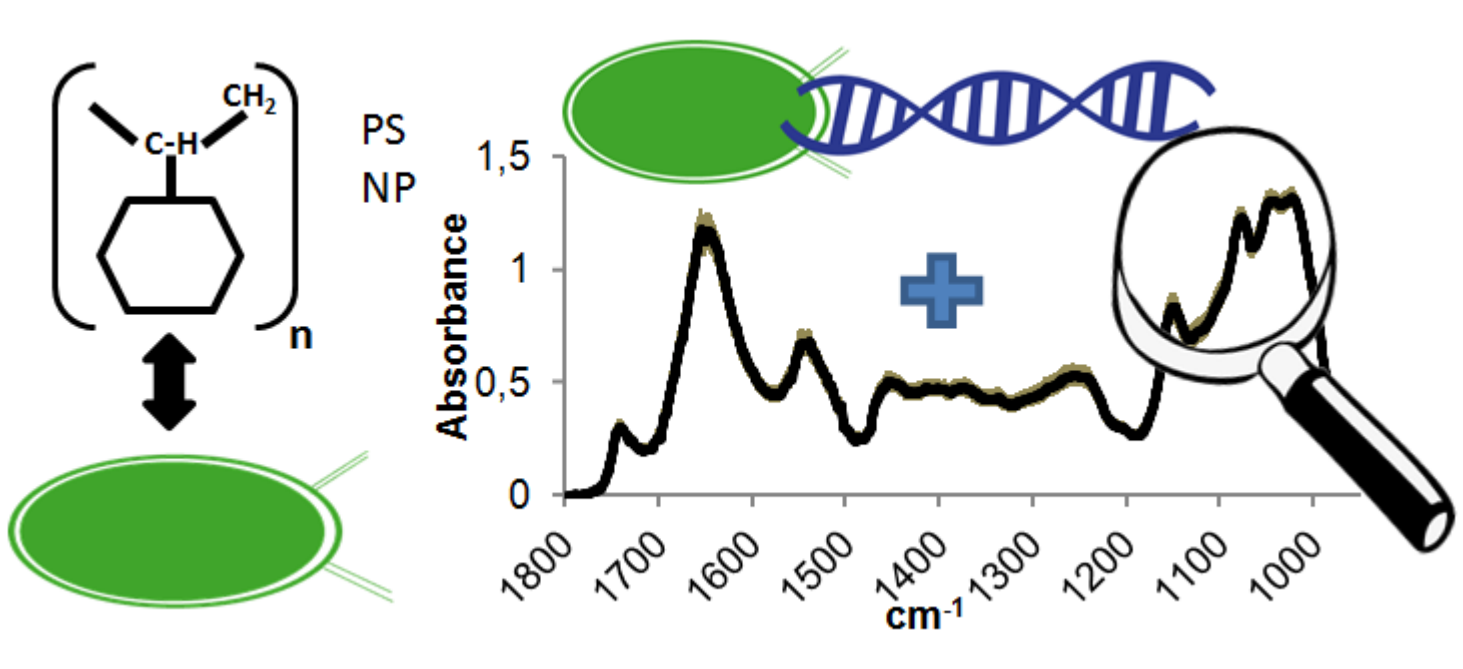
CH2
C-H
n
PS
NP
1,5
1
0,5
0
Absorbance
1800
1700
1600
1500
1400
1300
1200
1100
1000
cm-1